Asociación Argentina
de Mecánica Computacional

Mecánica Computacional Vol XXXII, págs. 1785-1797 (artículo completo)
Carlos G. García Garino, Aníbal E. Mirasso, Mario A. Storti, Miguel E. Tornello (Eds.)
Mendoza, Argentina, 19-22 Noviembre 2013

BUBBLE VELOCITY ENRICHMENT FOR EMBEDDED INTERFACES IN MULTI-FLUID FLOWS: A CRIME THAT DOES NOT PAY

Gustavo C. Buscaglia[a], **Roberto F. Ausas**[b], **Norberto Nigro**[c] **and Sergio R. Idelsohn**[d]

[a]*Instituto de Ciências Matemáticas e Computação, Universidade de São Paulo, Av. do Trabalhador Sãocarlense 400, 13560-970 São Carlos, SP, Brazil*

[b]*IBM Research, São Paulo, Brazil*

[c]*CIMEC-CONICET, Santa Fe, Argentina*

[d]*ICREA Research Professor, Centro Internacional de Métodos Numéricos en Ingeniería., Edificio C1, Campus Norte UPC C/ Gran Capitán S/N 08034 Barcelona, España*

Keywords: Multiphase flows, Embedded interfaces, Finite element method, Variational crime.

Abstract. We discuss ongoing work on the addition of a statically condensable bubble enrichment to capture kinks (surfaces where the function is continuous but its gradient exhibits a jump) in the velocity field at immersed interfaces not conforming with the element boundaries. Such kinks are frequent in multi-fluid flows because they arise whenever there are viscosity jumps or thermo-capillary effects. The enrichment is applied only at those elements of the finite element mesh cut by the interface, which is parameterized in this case with a level set function. The bubble function used in this work was introduced elsewhere (see Codina and Coppola-Owen, Int. J. Num. Meth. in Fluids 2005; 49:1287-1304) to capture discontinuities in the pressure gradient for two-phase flows, which arise because of density discontinuities under gravity. Its applicability as enrichment of the velocity field is not obvious due to a consistency error it creates in the variational formulation (the enrichment velocity fields are not in $H^1(\Omega)$, since they are discontinuous at some inter-element boundaries). In this work we assess the accuracy, robustness and limitations of this new enrichment in some problems involving interfaces. In its current form, the non-conformity of the bubbles introduces an unphysical numerical error which is of the same order as the interpolation error the bubbles are there to alleviate. Notice that these same bubble functions, when used for the pressure, do not lead to consistency error because they do belong to $L^2(\Omega)$.

1 INTRODUCTION

Consider the elliptic variational problem: *Find* $\varphi \in Z$ *such that*

$$\mathcal{B}(\varphi, \xi) = \mathcal{L}(\xi) \qquad \forall \xi \in Z \tag{1}$$

where $\mathcal{B}$ is a strongly coercive, continuous bilinear form on Z and $\mathcal{L} \in Z'$. The classical theory of finite elements (Ciarlet (1978); Brenner and L.R. (1994); Ern and Guermond (2004)) considers the discrete formulation: *Find* $\varphi_h \in Z_h$ *such that*

$$\mathcal{B}(\varphi_h, \xi_h) = \mathcal{L}(\xi_h) \qquad \forall \xi_h \in Z_h \tag{2}$$

for some Z_h contained in Z. It is then easily proved that

$$\|\varphi - \varphi_h\|_Z \leq C\,\|\varphi - \mathcal{I}_h\varphi\|_Z \tag{3}$$

where $\mathcal{I}_h\varphi$ is the Z_h-interpolant of the exact solution φ, and C is a constant independent of h.

When the exact solution is not regular the interpolation error $\|\varphi - \mathcal{I}_h\varphi\|_Z$ can be very large. To reduce it, new finite elements can be designed that are adapted to the specific problem at hand. When the new finite element space is not contained in Z it is called *non-conforming*, and its use cannot be justified by the classical theory. As coined by Gilbert Strang (Strang and Fix (2008)), the use of a $Z_h \not\subset Z$ constitutes a "variational crime" that has to be justified in terms of an extended theory, essentially contained in Strang's first and second lemmata (Ern and Guermond (2004)).

Some variational crimes are practically unpunished: (i) If the boundary conditions on Z_h are not the same as those on V but interpolants thereof, strictly speaking $Z_h \not\subset Z$. This is however of no consequence for the convergence rate of the approximation. (ii) The piecewise linear triangular element with the degrees of freedom at the midpoints of the edges is certainly not in $Z = H^1(\Omega)$. The standard formulation of the Poisson problem (with the integrals performed over the interiors of the triangles) is however convergent with the same rate as the conforming P_1 triangle. Variational crimes are frequently committed by finite element practitioners, and in many cases they are inconsequential. The purpose of this contribution is to discuss a variational crime that, though reasonable at first sight, ends up being harmful for the numerical approximation.

In the embedded interface treatment of multiphase flows there appear kinks in the velocity that limit the convergence of standard finite element spaces to $\mathcal{O}(\sqrt{h})$. The bubble function introduced by Coppola-Owen and Codina (2005) incorporates a kink in the approximation space and could thus be useful for obtaining more accurate approximations. It is restricted to each element and can be statically eliminated, which makes it attractive because the matrix structure does not depend on the interface location. Coppola-Owen and Codina applied this bubble function successfully to enrich the pressure space (density discontinuities produce kinks in the hydrostatic pressure), for which the variational formulation prescribes $L^2(\Omega)$ as exact space.

In this contribution we discuss the enrichment of the *velocity* space with this bubble function, which constitutes a *non-conforming* approximation since the associated space is *not* contained in the exact space for velocities $H^1(\Omega)$. A formal analysis of the consistency error shows that it is $\mathcal{O}(\sqrt{h})$, which precludes the bubbles from increasing the order of the method. Further, it is shown that the non-conforming space produces some awkward artifacts in the solution that make the conforming approximation preferrable.

2 MATHEMATICAL SETTING

2.1 Governing equations

We consider here the frequent case of two-fluid Newtonian flows. The fluid domain Ω is decomposed into a "plus" $(+)$ region and a "minus" $(-)$ region, separated by a *closed smooth* interface Γ, according to

$$\Omega \;=\; \Omega^+ \cup \Gamma \cup \Omega^- . \tag{4}$$

The physical properties (density ρ, viscosity μ) are assumed homogeneous and constant within each region, namely

$$(\rho(\mathbf{x}), \mu(\mathbf{x})) = \begin{cases} (\rho^+, \mu^+) & \text{if } \mathbf{x} \in \Omega^+ \\ (\rho^-, \mu^-) & \text{if } \mathbf{x} \in \Omega^- \end{cases} \tag{5}$$

where $\rho^\pm \geq 0$ and $\mu^\pm > 0$. The Cauchy stress tensor given by

$$\boldsymbol{\sigma} = -\,p\,\mathbb{I} + \mu\,(\nabla\mathbf{u} + \nabla\mathbf{u}^T), \tag{6}$$

with p the pressure, $\mathbb{I}$ the identity tensor and $\mathbf{u}$ the velocity, satisfies the dynamical equilibrium equation inside each region; i.e.,

$$\rho\mathbf{a} - \nabla\cdot\boldsymbol{\sigma} = \mathbf{b} \qquad \text{in } \Omega^+(t) \cup \Omega^-(t) \tag{7}$$

where $\mathbf{a}$ is the acceleration and $\mathbf{b}$ is a body force (such as gravity).

In addition to (7), the system is governed by the incompressibility condition

$$\nabla\cdot\mathbf{u} = 0 \qquad \text{in } \Omega^+ \cup \Omega^-, \tag{8}$$

and by the boundary conditions usually imposed to the Navier-Stokes equations, as for example

$$\mathbf{u}(\mathbf{x}) \;=\; \mathbf{u}_{\partial\Omega} \qquad \text{on } \partial\Omega, \tag{9}$$

and by the interface conditions at Γ discussed below.

2.2 Interface conditions

The simplest non-trivial interface behavior corresponds to capillary interfaces. Their are modeled by jump conditions for velocity and tractions at Γ given by

$$[\![\mathbf{u}]\!] \;=\; \mathbf{0} \tag{10}$$

$$[\![\boldsymbol{\sigma}\cdot\check{\mathbf{n}}]\!] \;=\; \gamma\,\kappa\,\check{\mathbf{n}} - \nabla_\Gamma\gamma \tag{11}$$

in which $[\![\cdot]\!]$ represents the jump of the quantity, e.g.;

$$[\![\mathbf{u}]\!](\mathbf{x}) \stackrel{\text{def}}{=} \mathbf{u}^+(\mathbf{x}) - \mathbf{u}^-(\mathbf{x}) \stackrel{\text{def}}{=} \lim_{\epsilon\to 0} \mathbf{u}(\mathbf{x} + \epsilon\,\check{\mathbf{n}}) - \lim_{\epsilon\to 0} \mathbf{u}(\mathbf{x} - \epsilon\,\check{\mathbf{n}}),$$

whereas γ is the surface tension, κ the mean curvature, $\check{\mathbf{n}}$ the normal to Γ (pointing towards Ω^+) and ∇_Γ the surface gradient. The reader is referred to Buscaglia and Ausas (2011) for details.

Equation (10) expresses that the fluids adhere to the interface on both sides. It implies in particular that incompressibility is satisfied (in the sense of distributions) at Γ; i.e., that the jump of the normal velocity $[\![\mathbf{u}\cdot\check{\mathbf{n}}]\!]$ vanishes. The motion thus preserves volume everywhere.

Equation (11) expresses the dynamical effect of the interface, which corresponds to a surface force over Γ. The tangential term, $\nabla_\Gamma \gamma$, appears in problems with inhomogeneous surface tension due to thermal or chemical gradients. It is known as Marangoni force.

Of main concern to us is the expected continuity of the field variables at the interface. Assuming the solution to be smooth on both sides of Γ, from (10) it is clear that $\mathbf{u}^+|_\Gamma = \mathbf{u}^-|_\Gamma$ and thus *the velocity field is continuous at* Γ. This in turn implies that *all tangential derivatives of* $\mathbf{u}$ *are also continuous at* Γ.

One can also prove that *the normal derivative* (∂_n) *of the normal component of the velocity is continuous at* Γ. To see this, decompose the velocity into normal and tangential components,

$$\mathbf{u} = \mathbf{u}_s + u_n \, \check{\mathbf{n}} \tag{12}$$

with $u_n = \mathbf{u} \cdot \hat{\mathbf{n}}$. The vector field $\hat{\mathbf{n}}$ is the normal extension of $\check{\mathbf{n}}$ to a neighborhood of Γ. The divergence of $\mathbf{u}$ can be written as the sum of a tangential term and a normal term as follows

$$\nabla \cdot \mathbf{u} = \partial_n \, u_n + \nabla_\Gamma \cdot \mathbf{u} \qquad \Rightarrow \qquad \partial_n \, u_n = -\nabla_\Gamma \cdot \mathbf{u}$$

and since the tangential derivative of $\mathbf{u}$ has already been shown to be continuous at Γ, so is $\partial_n u_n$.

The variables that are expected to be discontinuous at Γ are, thus, *the pressure and the normal derivative of the tangential velocity*.

2.3 Level set parameterization

We define the interface Γ as being the zero-level set of some function $\phi(\mathbf{x})$ which satisfies

$$\nabla \phi(\mathbf{x}) \neq 0 \qquad \forall \mathbf{x} \, \in \, \Gamma, \tag{13}$$

so that the normal to Γ,

$$\check{\mathbf{n}} = \frac{\nabla \phi}{\|\nabla \phi\|} \tag{14}$$

is well defined. This explains the plus/minus notation already introduced, since $\phi|_{\Omega^+} > 0$ and $\phi|_{\Omega^-} < 0$.

2.4 Variational formulation

The variational formulation adopted in this work can be found in Buscaglia and Ausas (2011) and is only briefly recalled here for completeness. Let V_∂ (respectively, V_0) be the velocity space consisting of fields in $H^1(\Omega)^d$ that satisfy the Dirichlet boundary conditions $\mathbf{u} = \mathbf{u}_{\partial\Omega}$ (respectively, $\mathbf{u} = \mathbf{0}$). Let also Q be the pressure space of functions in $L^2(\Omega)$, eventually restricted to have zero mean if velocity is imposed in the whole boundary $\partial\Omega$.

The exact problem thus reads: *Find* $(\mathbf{u}, p) \in V_\partial \times Q$ *such that*

$$\int_\Omega \rho \, (\mathbf{u} \cdot \nabla \mathbf{u}) \cdot \mathbf{v} \, d\Omega + \int_\Omega 2\mu \, D\mathbf{u} : D\mathbf{v} \, d\Omega - \int_\Omega p \, \nabla \cdot \mathbf{v} \, d\Omega =$$

$$= \int_\Omega \mathbf{b} \cdot \mathbf{v} \, d\Omega - \int_\Gamma \gamma \, (\mathbb{I} - \check{\mathbf{n}} \otimes \check{\mathbf{n}}) : D\mathbf{v} \, d\Gamma \tag{15}$$

$$\int_\Omega q \, \nabla \cdot \mathbf{u} \, d\Omega \;=\; 0 \tag{16}$$

$\forall(\mathbf{v}, q) \in V_0 \times Q$. Notice that for the surface tension a Laplace–Beltrami formulation is adopted (see e.g. Bänsch (2001); Ganesan et al. (2007); Gross and Reusken (2007); Buscaglia and Ausas (2011)) and that the symmetric gradient operator (i.e.; $D\mathbf{u} = \frac{1}{2}(\nabla\mathbf{u} + (\nabla\mathbf{u})^T)$) has been introduced.

3 FINITE ELEMENT APPROXIMATION

3.1 Discrete problem

The finite element formulation is based on the Algebraic Subgrid Scale method (see e.g. Codina (2001) and references therein). Since our formulation involves finite element interpolants which are discontinuous at Γ and also at some interelement boundaries, let us define an integral that avoids the discontinuities. More precisely, for a function f defined in Ω, for a given mesh $\mathcal{T}_h$ and for a given location Γ of the interface, let us denote

$$\int_{\square} f \, d\mathbf{x} \stackrel{\text{def}}{=} \sum_{K\in\mathcal{T}_h} \int_{K\setminus\Gamma} f \, d\mathbf{x} \tag{17}$$

In fact, it is this integral that is implemented in standard finite element codes, so that this notation has no practical consequences.

The discrete problem can now be written as: *Find* $\mathbf{u}_h$ *and* p_h*, belonging to* $V_{\partial h}$ *and* Q_h*, respectively, such that*

$$\begin{aligned}
\int_{\square} \boldsymbol{\mathcal{G}} \cdot \mathbf{v}_h \, d\mathbf{x} + \int_{\square} 2\mu D\mathbf{u}_h : D\mathbf{v}_h \, d\mathbf{x} - \int_{\square} p_h \nabla\cdot\mathbf{v}_h \, d\mathbf{x} + \int_{\Gamma} \gamma \, (\mathbb{I} - \check{\mathbf{n}}\otimes\check{\mathbf{n}}) : D\mathbf{v}_h \, d\Gamma + & \\
+ \int_{\square} \tau_h \, (\boldsymbol{\mathcal{G}} + \nabla p_h) \cdot (\mathbf{u}_h \cdot \nabla\mathbf{v}_h) \, d\mathbf{x} + \int_{\square} \zeta_h \, \nabla\cdot\mathbf{u}_h \, \nabla\cdot\mathbf{v}_h \, d\mathbf{x} &= 0 \qquad (18) \\
\int_{\square} q_h \, \nabla\cdot\mathbf{u}_h \, d\mathbf{x} + \int_{\square} \frac{\tau_h}{\rho} (\boldsymbol{\mathcal{G}} + \nabla p_h) \cdot \nabla q_h \, d\mathbf{x} &= 0 \qquad (19)
\end{aligned}$$

$\forall(\mathbf{v}_h, q_h) \in V_{0h} \times Q_h$, where

$$\boldsymbol{\mathcal{G}} = \rho\,(\mathbf{u}_h \cdot \nabla\mathbf{u}_h) - \mathbf{b}, \tag{20}$$

and the stabilization parameters are given by

$$\tau_h = \left[\frac{4\,\mu}{\rho\,h^2} + \frac{2\,\|\mathbf{u}_h\|}{h}\right]^{-1}, \quad \delta_h = 2\,\mu + \rho\,\|\mathbf{u}_h\|\,h \tag{21}$$

with h the local mesh size.

3.2 Velocity and pressure spaces

Let $P_1(\mathcal{T}_h)$ denote the classical, conforming P_1 space defined on the mesh $\mathcal{T}_h$. Defining the interface submesh

$$\mathcal{A}_h \stackrel{\text{def}}{=} \{K \in \mathcal{T}_h \,|\, K \cap \Gamma \neq \emptyset\} \tag{22}$$

the velocity/pressure combination proposed consists of the P_1/P_1 equal-order pair, enriched at each interface element with $d-1$ degrees of freedom for velocity:

$$\begin{aligned}
V_h &\stackrel{\text{def}}{=} (P_1(\mathcal{T}_h))^d \oplus \left\{ \sum_{K\in\mathcal{A}_h} \sum_{j=1}^{d-1} b^{(K,j)} \mathbf{B}^{(K,j)} \right\} \qquad (23) \\
Q_h &\stackrel{\text{def}}{=} P_1(\mathcal{T}_h) \qquad (24)
\end{aligned}$$

The second term on the right of (23) is the enrichment subspace (the span of the velocity bubbles), which will be denoted by E_h. The unknown coefficients $b^{K,j}$ ($j = 1$ in 2D, $j = 1, 2$ in 3D) can be eliminated at the element level because the associated basis functions $\mathbf{B}^{(K,j)}$ are *bubbles*. In other words, they vanish identically at elements other than the element K.

For the definition of the bubble functions we assume hereafter that the interface Γ is, or has been approximated by, a *planar facet* inside each element. Accordingly, the level set function ϕ is assumed to be a linear polynomial inside each element. The standard P_1 basis functions in each element will be denoted by N^j, $j = 1, \ldots, d + 1$.

Let ψ^K be the enrichment function introduced by Codina and Coppola-Owen to approximate the pressure in free-surface flows, defined by

$$\psi^K(\mathbf{x}) \stackrel{\text{def}}{=} \begin{cases} -\frac{1}{2}|\phi(\mathbf{x})| + \frac{1}{2}\sum_{j=1}^{d+1} |\phi(\mathbf{X}^j)| N^j(\mathbf{x}) & \text{if } \mathbf{x} \in K \\ 0 & \text{if } \mathbf{x} \notin K \end{cases} \tag{25}$$

This function is continuous inside K, linear on each side of Γ, and vanishes at the $d + 1$ vertices. Its gradient is discontinuous at Γ, which is useful to approximate functions with jumps in the *normal* derivative.

Following the discussion of the previous section, we use this function to enrich the *tangential velocity*. Taking an arbitrary basis $\check{\mathbf{t}}^1$ and $\check{\mathbf{t}}^2$ of the tangent space to Γ in K, that is, taking two (just one in 2D problems) linearly independent unit vectors satisfying

$$\check{\mathbf{n}} \cdot \check{\mathbf{t}}^j = 0 \qquad\qquad j = 1, \ldots, d - 1$$

we define

$$\mathbf{B}^{(K,j)}(\mathbf{x}) \stackrel{\text{def}}{=} \psi^K(\mathbf{x})\, \check{\mathbf{t}}^j \tag{26}$$

3.3 Discussion of the non-conformity variational crime

The formulation (18)-(19) is quite similar to a standard residual-stabilized formulation. However, because of the enrichment chosen for velocities, the discrete velocity fields are discontinuous at $\mathcal{F}_h$, defined as the set of faces (edges in 2D) crossed by Γ. This generates a *consistency error*, since the exact solution $(\mathbf{u}, p)$ *does not satisfy the discrete formulation (18)-(19)*.

Let us discuss the consistency error in the simplest case of an inertialess flow ($\rho = 0$), without surface tension ($\gamma = 0$) in the Galerkin formulation ($\tau_h = \delta_h = 0$). The problem fits into the abstract setting presented in the introduction, with

$$Z \stackrel{\text{def}}{=} (V, Q) = (H_0^1(\Omega)^d, L_0^2(\Omega)) \tag{27}$$

$$\varphi \stackrel{\text{def}}{=} (\mathbf{u}, p) \tag{28}$$

$$\xi \stackrel{\text{def}}{=} (\mathbf{v}, q) \tag{29}$$

$$Z_h \stackrel{\text{def}}{=} (V_h, Q_h) \tag{30}$$

$$\mathcal{B}(\varphi, \xi) \stackrel{\text{def}}{=} \int_\Box (2\,\mu\, D\mathbf{u} : D\mathbf{v} - \,p\,\nabla\cdot\mathbf{v} + \,q\,\nabla\cdot\mathbf{u})\; d\mathbf{x} \tag{31}$$

$$\mathcal{L}(\xi) \stackrel{\text{def}}{=} \int_\Box \mathbf{b}\cdot\mathbf{v}\; d\mathbf{x} \tag{32}$$

but now $Z_h \notin Z$. We assume that the bilinear form is continuous (with norm N) and uniformly weakly coercive on Z_h, namely that there exists a mesh-independent constant K such that

$$\sup_{\zeta_h \in Z_h} \frac{\mathcal{B}(\xi_h, \zeta_h)}{\|\zeta_h\|_\Box} \geq K\,\|\xi_h\|_\Box \qquad \forall\, \xi_h \in Z_h \tag{33}$$

where

$$\|\xi_h\|_\Box^2 = \int_\Box \left(\|\nabla \mathbf{v}_h(\mathbf{x})\|^2 + q_h^2(\mathbf{x})\right)\, d\mathbf{x}$$

Then we easily prove the *Second Strang Lemma*:

$$\|\varphi - \varphi_h\|_\Box \leq C\,\|\varphi - \mathcal{I}_h\varphi\|_\Box + \frac{1}{K}\sup_{\zeta_h\,\in\,Z_h}\frac{\mathcal{B}(\varphi,\zeta_h) - \mathcal{L}(\zeta_h)}{\|\zeta_h\|_\Box} \tag{34}$$

which splits the approximation error $\varphi - \varphi_h$ into an *interpolation error* (first term on the right) and a *consistency error* (second term on the right). The consistency error is a consequence of the non-conformity of the space. It vanishes identically if $Z_h \subset Z$. Further, for any $\zeta_h \in Z \cap Z_h$, it is clear that $\mathcal{B}(\varphi,\zeta_h) - \mathcal{L}(\zeta_h) = 0$.

Proof of Strang's lemma:

$$\begin{aligned}
\|\varphi - \varphi_h\|_\Box &\leq \|\varphi - \mathcal{I}_h\varphi\|_\Box + \|\mathcal{I}_h\varphi - \varphi_h\|_\Box \\
&\leq \|\varphi - \mathcal{I}_h\varphi\|_\Box + \frac{1}{K}\sup_{\zeta_h\,\in\,Z_h}\frac{\mathcal{B}(\mathcal{I}_h\varphi - \varphi_h,\zeta_h)}{\|\zeta_h\|_\Box} \\
&\leq \|\varphi - \mathcal{I}_h\varphi\|_\Box + \frac{1}{K}\sup_{\zeta_h\,\in\,Z_h}\frac{\mathcal{B}(\mathcal{I}_h\varphi - \varphi + \varphi - \varphi_h,\zeta_h)}{\|\zeta_h\|_\Box} \\
&\leq \left(\frac{N}{K} + 1\right)\|\varphi - \mathcal{I}_h\varphi\|_\Box + \frac{1}{K}\sup_{\zeta_h\,\in\,Z_h}\frac{\mathcal{B}(\varphi - \varphi_h,\zeta_h)}{\|\zeta_h\|_\Box} \\
&= \left(\frac{N}{K} + 1\right)\|\varphi - \mathcal{I}_h\varphi\|_\Box + \frac{1}{K}\sup_{\zeta_h\,\in\,Z_h}\frac{\mathcal{B}(\varphi,\zeta_h) - \mathcal{L}(\zeta_h)}{\|\zeta_h\|_\Box} \quad \Box
\end{aligned}$$

If the discrete space Z_h interpolates the exact solution with order $\mathcal{O}(h^p)$, the convergence of the numerical methods only depends on the behavior, as h tends to zero, of the consistency error

$$C_h = \sup_{\zeta_h\,\in\,Z_h}\frac{\mathcal{B}(\varphi,\zeta_h) - \mathcal{L}(\zeta_h)}{\|\zeta_h\|_\Box}$$

It is an interesting exercise of finite element consistency analysis to try to estimate C_h for our specific formulation. We begin by noticing that we can always decompose

$$\zeta_h = (\mathbf{v}_h, q_h) = (\mathbf{v}_h^c + \mathbf{v}_h^{nc}, q_h) = (\mathbf{v}_h^c, q_h) + (\mathbf{v}_h^{nc}, 0) = \zeta_h^c + \zeta_h^{nc}$$

where $\mathbf{v}_h^c$ belongs to $P_1(\mathcal{T}_h)^d$ (the conforming part of $\mathbf{v}_h$) and $\mathbf{v}_h^{nc}$ belongs to E_h (the non-conforming, bubble part of $\mathbf{v}_h$). Because the conforming part of ζ_h has zero consistency error, we have

$$\begin{aligned}
\mathcal{B}(\varphi,\zeta_h) - \mathcal{L}(\zeta_h) &= \mathcal{B}((\mathbf{u},p),(\mathbf{v}_h^{nc},0)) - \mathcal{L}((\mathbf{v}_h^{nc},0)) \\
&= \int_\Box (2\,\mu\, D\mathbf{u} : D\mathbf{v}_h^{nc} - p\,\nabla\cdot\mathbf{v}_h^{nc} - \mathbf{b}\cdot\mathbf{v}_h^{nc})
\end{aligned}$$

One now integrates by parts the viscous and pressure terms, which leads to integrals of the jump of $\boldsymbol{\sigma}\cdot\check{\mathbf{n}}$ over the element boundaries and over Γ, i.e.,

$$\mathcal{B}(\varphi,\zeta_h) - \mathcal{L}(\zeta_h) = -\int_\Box (\nabla\cdot\boldsymbol{\sigma} + \mathbf{b})\cdot\mathbf{v}_h^{nc}\,d\mathbf{x} + \int_\Gamma [\![(\boldsymbol{\sigma}\cdot\check{\mathbf{n}})\cdot\mathbf{v}_h^{nc}]\!] + \sum_{\text{edges }e_h}\int_{e_h}[\![(\boldsymbol{\sigma}\cdot\check{\mathbf{n}})\cdot\mathbf{v}_h^{nc}]\!]$$

The first term is identically zero because $\nabla \cdot \boldsymbol{\sigma} + \mathbf{b} = 0$. The second term also vanishes identically because $\mathbf{v}_h^{nc}$ is continuous across Γ, so that

$$[\![(\boldsymbol{\sigma} \cdot \check{\mathbf{n}}) \cdot \mathbf{v}_h^{nc}]\!] = [\![(\boldsymbol{\sigma} \cdot \check{\mathbf{n}})]\!] \cdot \mathbf{v}_h^{nc}$$

which is zero because $[\![(\boldsymbol{\sigma} \cdot \check{\mathbf{n}})]\!] = 0$ across any surface contained in Ω. It only remains the third term, which also vanishes at all edges (i.e., element boundaries) e_h where $\mathbf{v}_h^{nc}$ is continuous. This leaves the set of edges crossed by the interface, $\mathcal{F}_h$, as the only source of consistency error,

$$\mathcal{B}(\varphi, \zeta_h) - \mathcal{L}(\zeta_h) \;=\; \sum_{e_h \in \mathcal{F}_h} \int_{e_h} (\boldsymbol{\sigma} \cdot \check{\mathbf{n}}) \cdot [\![\mathbf{v}_h^{nc}]\!]$$

Notice that $\mathcal{F}_h$ is a "rough" surface determined by the mesh, and that

$$\mathrm{meas}(\mathcal{F}_h) \leq c\, \mathrm{meas}(\Gamma)$$

In principle $\boldsymbol{\sigma}$ is arbitrary, and the normal $\check{\mathbf{n}}$ jumps from one e_h to the other, so that little can be done with the expression above other than

$$\mathcal{B}(\varphi, \zeta_h) - \mathcal{L}(\zeta_h) \leq \|\boldsymbol{\sigma}\|_\infty \sum_{e_h \in \mathcal{F}_h} \int_{e_h} \| [\![\mathbf{v}_h^{nc}]\!] \|$$

The function $\mathbf{v}_h^{nc}$ is a linear combination of piecewise linear bubbles that vanish at the nodes. We thus have, assuming $d = 2$,

$$\mathbf{v}_h^{nc} = \sum_{K \in \mathcal{A}_h} b^{(K)}\, \mathbf{B}^{(K)}$$

and

$$\sum_{e_h \in \mathcal{F}_h} \int_{e_h} \| [\![\mathbf{v}_h^{nc}]\!] \| \leq 2 \sum_{K \in \mathcal{A}_h} |b^{(K)}| \int_{\partial K} \|\mathbf{B}^{(K)}\| = 2 \sum_{K \in \mathcal{A}_h} |b^{(K)}| \int_{\partial K} \|\psi^K\| \tag{35}$$

It is easy to check that $\int_{\partial K} \|\psi^K\| \leq h_K^2$ so that

$$\mathcal{B}(\varphi, \zeta_h) - \mathcal{L}(\zeta_h) \leq 2\, \|\boldsymbol{\sigma}\|_\infty\, h^2 \sum_{K \in \mathcal{A}_h} |b^{(K)}| \tag{36}$$

Now, let us estimate

$$\|\zeta_h^{nc}\|_\square^2 = \sum_{K \in \mathcal{A}_h} \int_K \|\nabla \mathbf{v}_h^{nc}\|^2$$

noticing that, if the distance from Γ to a vertex is δ_K, then $\max |\psi^K| \simeq \delta_K$ and

$$\int_K \|\nabla \mathbf{v}_h^{nc}\|^2 = |b^{(K)}|^2 \int_K \|\nabla \psi^K\|^2 \simeq c'\, |b^{(K)}|^2\, h_K^2 \tag{37}$$

where we have assumed that h_K/δ_K is bounded (possibly perturbing the mesh). As a consequence,

$$\frac{\mathcal{B}(\varphi, \zeta_h^{nc}) - \mathcal{L}(\zeta_h^{nc})}{\|\zeta_h^{nc}\|_\square} \leq c\, \|\boldsymbol{\sigma}\|_\infty\, h^2 \frac{\sum_{K \in \mathcal{A}_h} |b^{(K)}|}{\left(\sum_{K \in \mathcal{A}_h} |b^{(K)}|^2\, h_K^2\right)^{\frac{1}{2}}}$$

which using the discrete Cauchy-Schwartz inequality, assuming $h_K \simeq h$ for all K and noting that $\sum_{K\in\mathcal{A}_h} 1 \simeq \mathrm{meas}(\Gamma)/h$, leads to

$$\frac{\mathcal{B}(\varphi,\zeta_h^{nc}) - \mathcal{L}(\zeta_h^{nc})}{\|\zeta_h^{nc}\|_\square} \leq c\,\|\boldsymbol{\sigma}\|_\infty\ \mathrm{meas}(\Gamma)^{\frac{1}{2}}\ h^{\frac{1}{2}} \tag{38}$$

and this last expression, though not rigorously, is expected to be a reasonable estimate for the consistency error C_h.

$$C_h \sim c\,\|\boldsymbol{\sigma}\|_\infty\ \mathrm{meas}(\Gamma)^{\frac{1}{2}}\ h^{\frac{1}{2}} \tag{39}$$

This formal calculation thus suggests that the order of the consistency error is $\mathcal{O}(\sqrt{h})$, i.e., *the same order of the interpolation error that the bubbles were designed to improve*.

Nevertheless, sometimes two approximations converge with the same order but have completely different accuracies. Also, some errors are more unphysical than others, even if the orders coincide. This is assessed in the next section by numerical experimentation. Some peculiarities of the numerical behavior can already be deduced from (39).

Arguably, the dominant error of the conforming, piecewise P_1 formulation comes from the velocity interpolation error at the interface elements. In turn, this error arises due to kinks in the tangential velocity gradient. One expects the error to be the same for two problems which only differ by a uniform shift in the pressure field. However, for the non-conforming enriched formulation one obtains in (39) that the whole Cauchy stress tensor intervenes in the error, not just its viscous part, so that two exact solutions that differ by a constant pressure will be approximated differently. This already suggests that the error must behave rather unphysically.

4 NUMERICAL EXPERIMENT

The simplest test we can perform to numerically show this consistency error is the Couette flow between parallel walls. In this example we consider a square channel with a horizontal interface separating the two fluids having different viscosities. The problem setting and boundary conditions are shown in figure 1. The exact solution for this problem is *exactly* interpolated by the enriched space (the interpolation error is *zero*), so that in the Second Strang Lemma (34) only the consistency error survives. Were it not for the "crime" committed, the exact solution would be retrieved. Unfortunately, from the last section we expect a total error of the same order as that of the unenriched formulation, it only remains to assess numerically the actual value of the error.

The exact solution reads

$$u_1(x_1,x_2) = \begin{cases} a\,\frac{x_2}{\ell} & \text{if } x_2 < \ell \\ a + (1-a)\,\frac{x_2-\ell}{1-\ell} & \text{if } x_2 \geq \ell \end{cases} \tag{40}$$

$$u_2(x_1,x_2) = 0 \tag{41}$$

$$p(x_1,x_2) = \bar{p} \tag{42}$$

where $\bar{p}$ is a constant, ℓ is the interface position, μ_1 and μ_2 are the fluid viscosities and a is defined as

$$a = \frac{\ell\,\mu_2}{(1-\ell)\,\mu_1 + \ell\,\mu_2} \tag{43}$$

From (40)-(41) the velocity is continuous at Γ but its gradient is discontinuous. We solve this problem with $\ell = 0.4$, $\mu_1 = 1$, $\mu_2 = 10$ and $\bar{p} = 100$. A sequence of unstructured meshes is built of which the first one consists of 64 elements. To this mesh we assign a mesh size $h = 0.145$. The following six meshes in the sequence are built by subdivision. We measure the velocity error in the $H^1(\Omega)$-norm and the pressure error in the $L^2(\Omega)$-norm using the enrichment and without using it. The results are plotted in figure 2 and 3. As shown in these figures the pressure and the velocity error norms converge with order $\mathcal{O}(h^{\frac{1}{2}})$ as expected in both cases. For the case with the enrichment, the magnitude of these errors is much larger.

For illustration purposes figure 4 shows contours of the pressure field and contours of the vertical component of the velocity field for the fourth mesh in the sequence. Remember that the exact solution corresponds to a constant pressure $\bar{p} = 100$ and a zero vertical velocity $u_2 = 0$. For both cases, the oscillations near the interface are quite noticeable, and they are much more pronounced when the enrichment is used. In particular, the error of the enriched formulation depends on the value of the (uniform!) pressure $\bar{p}$, and the *amplitude* of the oscillations roughly scales with $|\bar{p}|$. The unenriched formulation has oscillations that are strictly independent of $|\bar{p}|$.

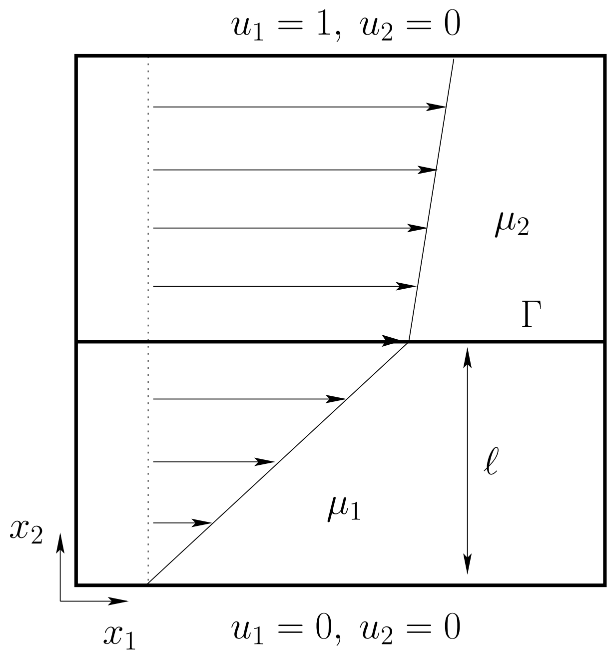

Figure 1: Problem setting for the Couette flow to numerically assess the consistency error of the formulation with the enrichment.

5 CONCLUSIONS

We have presented preliminary results on the theoretical and numerical assessment of a variational crime in incompressible multi-fluid finite element formulations. The proposed crime consists of adding bubbles that improve the interpolation properties of the velocity space at the expense of violating the consistency of the formulation (the exact solution no longer satisfies the discrete formulation).

Many variational crimes from the literature either are harmless, or decrease the convergence order, or lead to ill-posed discrete formulations altogether. In this case, interestingly, the consistency error ends up being of the same order as the interpolation error of the “legal” formulation. However, it ends up not being convenient because it introduces some kind of zero-stress condition (weakly) at the interface, which is completely unphysical.

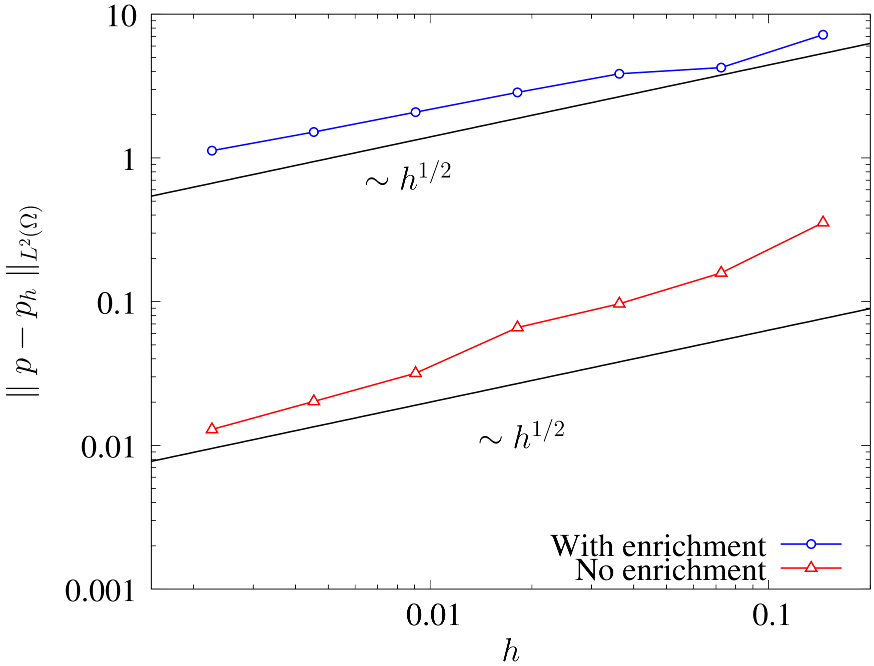

Figure 2: $L^2(\Omega)$ error norm of the pressure field for the Couette problem using the enrichment (circles) and without the enrichment (triangles).

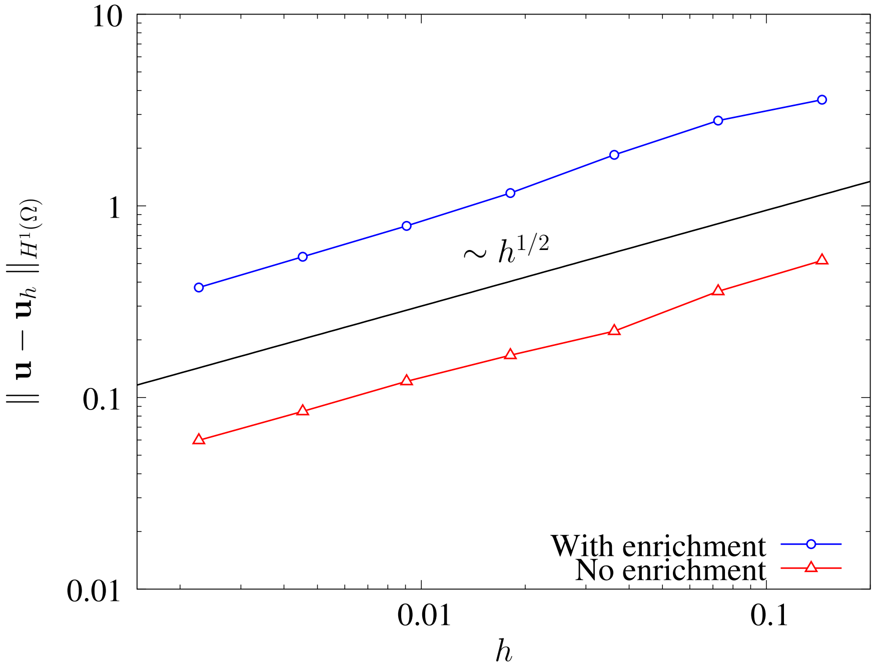

Figure 3: $H^1(\Omega)$ error norm of the velocity field for the Couette problem using the enrichment (circles) and without the enrichment (triangles).

The method could perhaps be applicable in flows in which one of the fluids is much less viscous and less dense than the other, in which case the interface can be quasi-stress-free (assuming zero reference pressure).

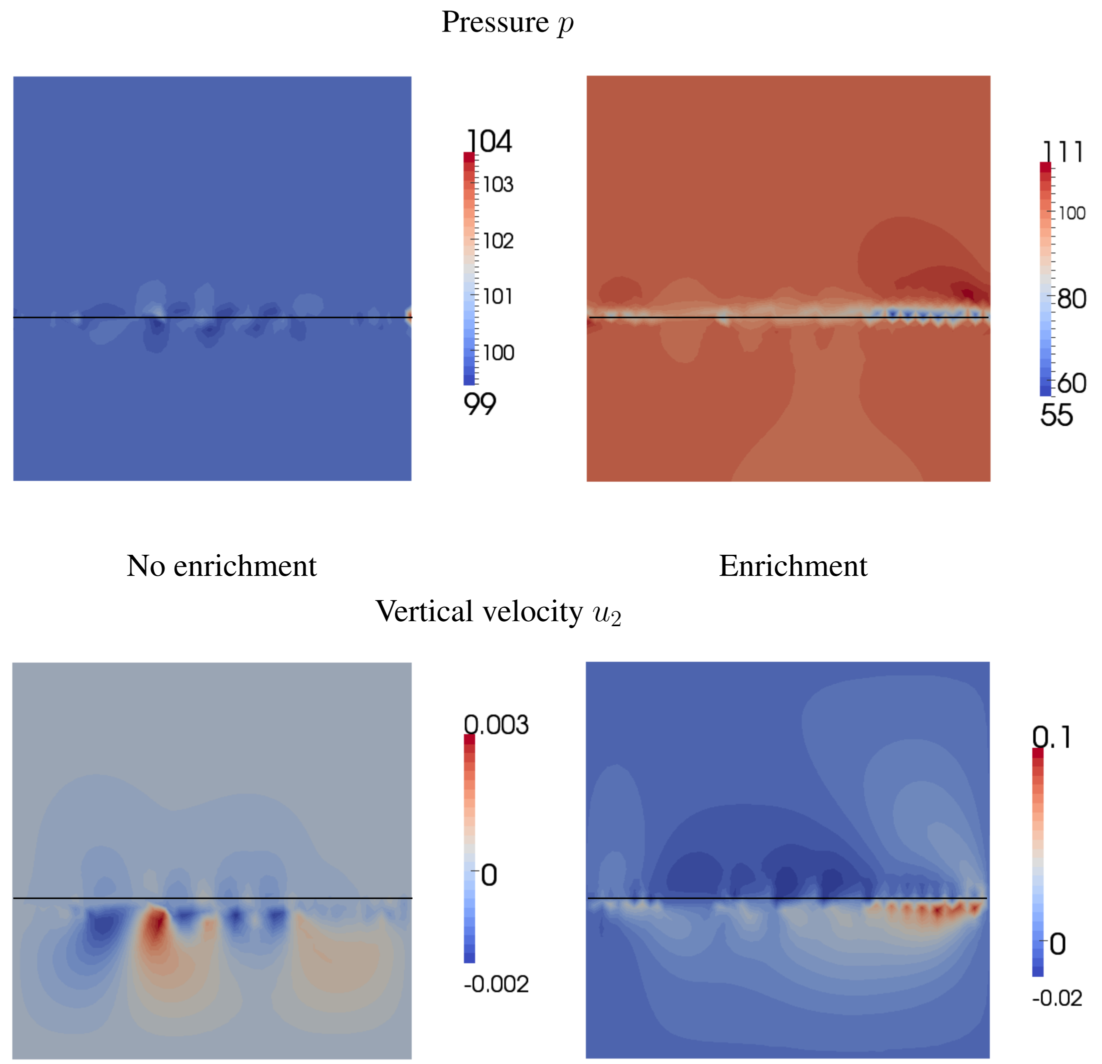

Figure 4: Contours of pressure (top) and vertical velocity (bottom) for the Couette problem without using the enrichment (left) and with the enrichment (right).

Current work aims at developing some variant of the method discussed above which circumvents its unphysical behavior while preserving its interpolation properties and its simplicity (with respect to XFEM or GFEM). The main difficulties seem to come from the (natural) boundary condition on the total stress that appears at the non-conformity element faces. Experiments are being performed on switching to a formulation in which the pressure gradient is not integrated by parts, and will be reported in the near future.

ACKNOWLEDGMENTS

The authors gratefully acknowledge partial support from FAPESP and CNPq (Brazil) and from CONICET (Argentina).

REFERENCES

Bänsch E. Finite element discretization of the Navier–Stokes equation with a free capillary surface. *Numer. Math.*, 88:203–235, 2001.

Brenner S. and L.R. S. *The Mathematical Theory of Finite Element Methods*. Springer, 1994.

Buscaglia G. and Ausas R. Variational formulations for surface tension, capillarity and wetting. *Computer Meth. Appl. Mech. Engng.*, 200:3011–3025, 2011.

Ciarlet P. *The finite element method for elliptic problems*. North-Holland, 1978.

Codina R. A stabilized finite element method for generalized stationary incompressible flows. *Comput. Methods Appl. Mech. Engrg.*, 190:2681–2706, 2001.

Coppola-Owen A.H. and Codina R. Improving eulerian two–phase flow finite element approximation with discontinuous gradient pressure shape functions. *Int. J. Numer. Meth. Fluids*, 49:1287–1304, 2005.

Ern A. and Guermond J.L. *Theory and practice of finite elements*. Springer, 2004.

Ganesan S., Matthies G., and Tobiska L. On spurious velocities in incompressible flow problems with interfaces. *Comput. Methods Appl. Mech. Engrg.*, 196:1193–1202, 2007.

Gross S. and Reusken A. Finite element discretization error analysis of a surface tension force in two-phase incompressible flows. *SIAM J. Numer. Anal.*, 45:1679–1700, 2007.

Strang G. and Fix G. *An analysis of the finite element method*. Wellesley-Cambridge Press, Wellesley, MA, second edition, 2008.